

# NEW BEAM POSITION MONITORS FOR THE CERN LINAC3 TO LEIR ION BEAM TRANSFER LINE

G. Baud, M. Bozzolan, R. Scrivens, L. Søby  
 CERN, 1211, Geneva, Switzerland

## Abstract

The ion injection line into the CERN Low Energy Ion Ring (LEIR) has recently been equipped with nine, new, electrostatic Beam Position Monitors (BPMs) in order to measure and optimize the trajectory of the low intensity ion beams coming from Linac3. In this paper, we describe the design of the BPM, the low noise charge amplifier mounted directly on the BPM, and the digital acquisition system. There is special emphasis on the first commissioning results where the measured beam positions were perturbed by EMI and charging of the BPM electrodes by secondary particles. The effect of mitigation measures, including repelling voltages on the electrodes and external magnetic fields, are also discussed.

## INTRODUCTION

The CERN Linac3 provides heavy ions, mainly Pb<sup>54+</sup> at an energy of 4.2MeV/u, to the Low Energy Ion Ring (LEIR). Here the ions (pulses of up to 30μA, 200μs) are accelerated to 72MeV/u, extracted to the PS and further to the SPS where the fully stripped ions are either extracted for fixed target physics, or transferred to the LHC for ion collisions. In order to optimize the injection efficiency into LEIR, the transfer line between Linac3 and LEIR has recently been equipped with nine highly sensitive electrostatic BPMs (Figure 1).

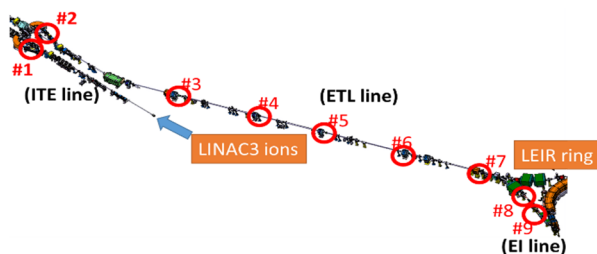


Figure 1: Linac3 to LEIR transfer line BPM layout.

## BPM DESIGN

Table 1 summarises the BPM system specifications.

Table 1: BPM Specifications

Parameter	Value	Comment
Accuracy	0.5mm	-
Resolution	0.2mm	For 4uA current
Time resolution	1us	Along 200us pulse
Max. Beam displ.	±15 mm	-
Max beam current	50uA	-
Nb. of injections	1-13	Every 100-200ms

The BPMs are of a dual plane electrostatic type with an aperture of 196mm and a length of 200mm. The azimuthal width of the electrodes is 75° and the distance to ground is 21.5mm. The ~20pF electrodes are connected to high impedance charge amplifiers mounted directly onto the BPM body, via 75Ω cables, see Figure 2. The transfer impedance is about 30Ω yielding an electrode signal of ~0.1mV for a centred beam. All parts are of 316 LN stainless steel. The two BPMs nearest the LEIR ring have a non-evaporable getter (NEG) coating on the chamber walls to lower the overall vacuum level in this region.

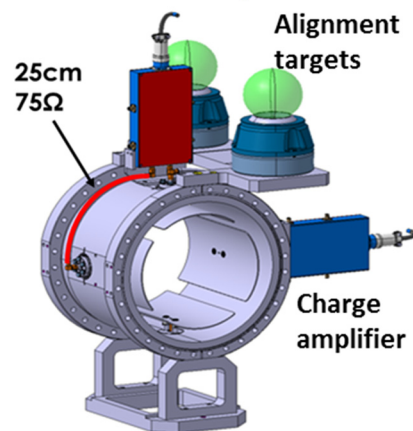


Figure 2: 3D model of the BPM.

## ACQUISITION SYSTEM

### Electronics

The input stage of the front-end electronics mounted directly on the BPMs is a charge amplifier. Gain calibration is performed by injecting a known charge into each input through a low capacitance calibration capacitor (1pF). After charge amplification, further amplifier stages generate the sum ( $3 \times 10^{12}$  V/C gain) and difference ( $6 \times 10^{12}$  V/C gain) signals. The -3dB bandwidth is 60Hz to 2MHz. A more detailed description of the head amplifier can be found in [1]. Coaxial cables transmit the signals to the control room where commercial, 8 channel, 12 bit Analogue to Digital Converters (ADCs) sample the signals.

### Front-End Software: FESA

The Front-End Software Architecture (FESA) is a C++ framework used at CERN to design, develop, test and deploy real-time control software. It is used to provide software control and monitoring of the acquisition triggers, data read-out, processing and calibration. It also allows the data to be easily integrated with standard tools such as the beam steering Graphical User Interface (GUI) or long-term logging database.

Content from this work may be used under the terms of the CC BY 3.0 licence (© 2018). Any distribution of this work must maintain attribution to the author(s), title of the work, publisher, and DOI.

For each LEIR cycle of 2.4 or 3.6 seconds, depending on the configuration, the FESA class prepares the ADCs, and starts the acquisition 200 $\mu$ s before each LEIR injection. 4096 samples at a sampling rate of 6.125 MHz are captured, corresponding to a 650 $\mu$ s time period centred on the 200 $\mu$ s Linac pulse. These are then read-out 10ms after each injection trigger.

As the acquisition system is linear, positions are computed using a simple scaling of the difference/sum ratio of electrode signals. Various algorithms are available to provide instantaneous or average positions. Providing the position at the end of the pulse proved to be particularly useful to counter the baseline drifts discussed in the following sections.

## BEAM MEASUREMENTS

The two first BPMs were installed in the ITE line at the beginning of 2017, and tested during the 2017 run with Ar<sup>11+</sup> beams. The remaining seven BPMs were installed at the beginning of 2018 with all nine BPMs now used to measure nominal Pb<sup>54+</sup> beams. The signals from the first beam tests showed perturbations due to both EMI and low energy secondary particles hitting the electrodes.

### EMI from Quadrupoles

Figure 3 shows the perturbation of the baseline observed close to the start of the Linac pulse. This perturbation was found to be due to a nearby, pulsed quadrupole creating ground currents that ran along the screen of the coaxial input cables to the front-end amplifiers. By adding high mu toroidal cores around these cables, this interference was completely suppressed.

### Secondary Particles

Even though the aperture of the first BPM is nearly twice that of the neighbouring vacuum chambers the electrode signals were found to be completely saturated. While the signals from the second BPM did not enter saturation, they clearly showed a baseline drift along the beam pulse. An example is given in Figure 3, which also shows the baseline distortion due to EMI before the beam passage.

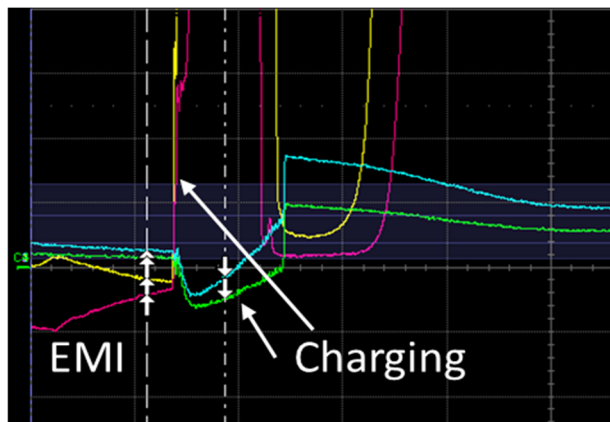


Figure 3: Horizontal and vertical sum signals from the first two BPMs in the ITE line. Yellow /Blue: BPM1/BPM2 horizontal sum. Purple/Green: BPM1/BPM2 vertical sum.

Simulating a continuous negative charging of the electrodes during the beam passage, as shown Figure 4, one obtains a result similar to what is observed in Figure 3, indicating that secondary electrons are directly impacting on the electrodes.

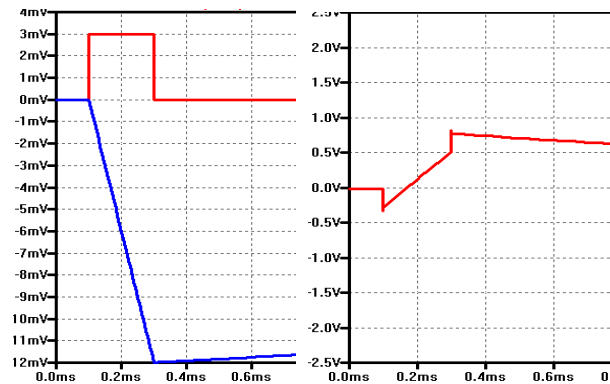


Figure 4: Left: Square 200us beam pulse (red) and continuous charging by electrons (blue). Right: Result of summation of the two signals and amplification.

### Repelling Potential on Electrodes

Suspecting secondary electrons either from ionisation of the rest gas or desorption from the vacuum chamber, the front-end electronics was modified to enable a repelling voltage to be added on each electrode. This significantly improved the quality of the observed signals (see Figure 5). When scanning the repelling voltages, it is usually possible to find a setting where the primary beam pulse signal is unaffected by charging (in this case close to -4V). Further increasing the voltage results in positive charging of the electrodes (amplifier response is inverted), which we believe is due to the attraction of ions from the rest gas ionisation. Unfortunately, this ideal repelling potential is different for each electrode and was seen to depend on both beam and Linac parameters. This was therefore not a final mitigation for this issue.

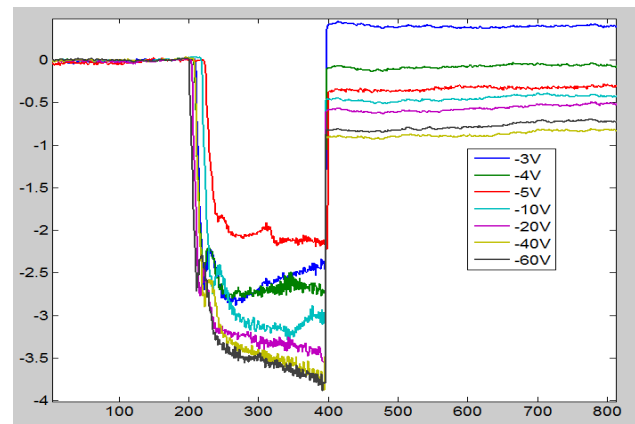


Figure 5: Electrode charging as function of repelling voltage.

## Solenoids and Dipoles

A series of iterations with simulations (see later) and installations of low field solenoids and dipoles around or close to the BPMs confirmed the presence of secondary electrons ( $<100\text{eV}$ ) generated close to the BPM. At present, all but one of the BPMs have been equipped with solenoids as shown in Figure 6. Combining this solenoid field with the clearing voltage on the electrodes allowed saturation to be avoided on all BPMs and enabled a measurement of the beam position to be performed at one single point at the end of the pulse (see Fig. 7). This is adequate for steering the beam along the transfer line. However, measurements along the pulse, important to tune the source and RF parameters, are still not possible as the form of the charging profile is unknown.

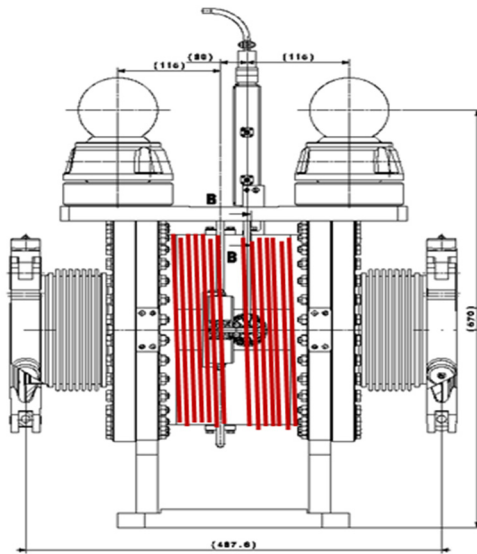


Figure 6: BPM with solenoid

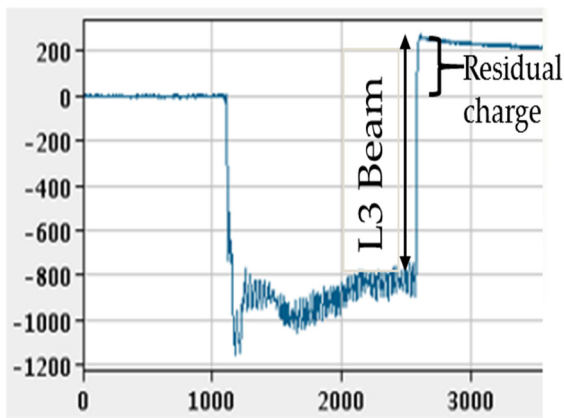


Figure 7: Sum signal from one BPM equipped with both solenoid and electrode bias. The residual charge caused by electrode charging is visible as a baseline shift at the end of the pulse.

## SIMULATIONS

In order to understand the source of the secondary particles and how the suppression schemes work, simulations were performed using the IBSIMU code [2]. A simplified

geometry was constructed, including the vacuum chamber and the four separated electrodes of the BPM, which can be electrically biased. Magnetic fields generated by solenoids or dipoles are then imported into the simulation.

Secondary particles are generated as either:

- secondary electrons from the walls, with an energy distribution based on [3] for the creation of low energy electrons ( $<100\text{eV}$ )
- protons and electrons from the center of the vacuum chamber in order to represent residual gas ionization.

The pressure in the line is below  $10^{-8}$  mbar. The beam density is low enough that space charge fields can be neglected. For simplicity, secondary particles from the beam pipe are emitted normally to the vacuum chamber, and at  $\pm 45^\circ$  to the wall normal.

Images of the tracked secondary particles are shown in Figure 8 for a solenoid field of  $0.6\text{mT}$  and an electrode bias voltage of  $-5\text{V}$ . In such a configuration we see that only a small number of wall-emitted electrons can strike the electrodes, whereas a higher fraction of ions from the gas can reach the electrodes. Electrons from rest gas ionization are not shown and do not reach the BPM electrodes.

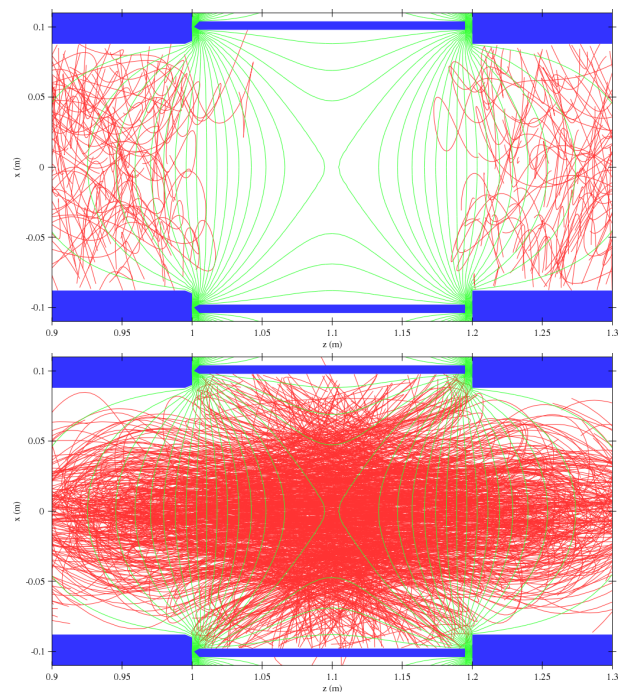


Figure 8: Secondary particle tracks in the simulation, with an applied magnetic field from a solenoid along the beam axis. Top: Electrons emitted from the vacuum chamber walls. Bottom: Ions Generated from the gas ionization. Blue: Vacuum chamber and electrodes. Red: Secondary particle tracks. Green: Equipotentials of the electrode bias voltage.

Expected production rates for secondary particles from the walls depends on local losses of a small fraction of the beam (the loss rate along the line is on average  $10^{-3}$  per meter), and the production of gas ions depends on the local pressure (which can vary along the transfer line). The production of secondaries from the two processes can there-

Content from this work may be used under the terms of the CC BY 3.0 licence (© 2018). Any distribution of this work must maintain attribution to the author(s), title of the work, publisher, and DOI.

fore be scaled to fit the measurements at each BPM location. Figure 9 shows a comparison of simulation and measurements as a function of the applied solenoid field, which is seen to be in agreement. In this case the second BPM (right plot) is subject to three times as many secondary particles as the first (left plot). These simulations, however, predict a fully symmetric collection of secondary particles by all four electrodes, whereas measurements typically show a strong asymmetry, which might be due to factors such as asymmetric loss pattern or the influence of nearby magnetic components. The result is that it has not been possible to find magnetic and electric field distributions that can suppress the secondaries on all electrodes simultaneously. A fully reliable beam position measurement as a function of time in the beam pulse has therefore not been achieved.

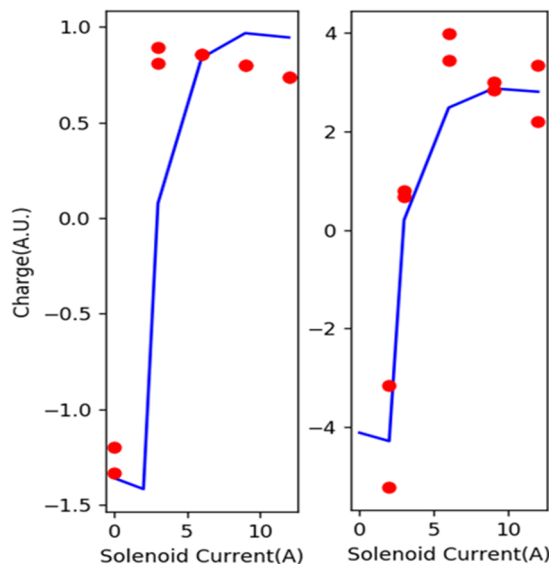


Figure 9: Collected charge on BPM electrodes as a function of the applied solenoid current (0.2mT/Ampere) and electrode repelling voltage of -5V. Red dots show measurements of collected charge summed on all four electrodes. The blue line is the simulated collected charge. Left and right plots correspond to two different BPMs, based on the same simulation.

## HIGH FREQUENCY ACQUISITION

The bunching frequency of the Linac is 101.3MHz, with a complete de-bunching expected at the end of the transfer line due to the energy spread. A BPM acquisition system at this frequency was therefore not initially pursued, leading to the development of the baseband system described above. However, after having modified one of the front-end amplifiers to transmit this higher frequency part of the beam spectrum, it was seen that sufficient bunching is still present at the last BPM before injection into LEIR for position measurements. The signals in Figure 10 were obtained using an 8-bit oscilloscope running at 500MS/s and a Matlab script performing a 2MHz bandpass filter and AM demodulation. Computing the position from this last BPM in the transfer line yields a position resolution along the

pulse of better than 0.5mm when averaged over 5 $\mu$ s. Such a measurement is completely insensitive to the slow charging of the electrodes by secondary particles. The signal to noise ratio is dominated by the 8-bit oscilloscope and a dedicated acquisition system is therefore expected to perform significantly better. Such a system is currently being constructed to overcome the issues observed with the baseband acquisition.

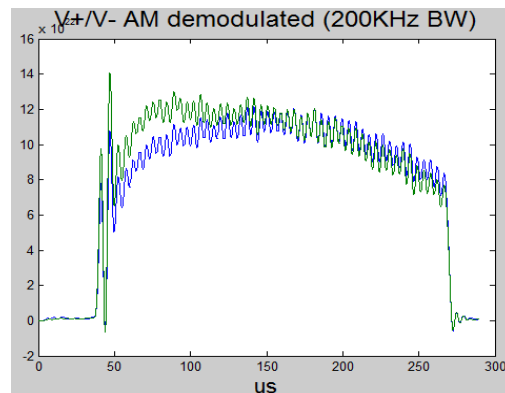


Figure 10: Electrode signals after filtering and AM demodulation.

## CONCLUSION

Nine electrostatic BPMs have been installed in the Linac3 to LEIR transfer line with the aim of being able to measure the beam position along the 200 $\mu$ s beam pulse. The signals from all the BPMs but one showed significant charging of the electrodes by secondary particles, which subsequent simulations showed were mainly electrons emitted from the chamber walls, but also ions from rest gas ionisation. Different configurations of electrode bias voltages and external magnetic fields significantly improves the signal quality but cannot guarantee a correct position measurement along the beam pulse, with only a single point measurement at the end of the pulse reliably used during operation.

A new system, using the 101MHz bunching component of the Linac, which has been shown to be present even at the last BPM, is insensitive to the slow charging of the electrodes and will now be implemented to provide beam position measurements along the pulse.

## ACKNOWLEDGEMENTS

We would like to thank F. Guillot-Vignot and B. Moser for their help during the installation phases of the BPMs and the installation of magnets.

## REFERENCES

- [1] L. Søby *et al*, ELENA orbit and Schottky measurement systems, in *Proc. of IPAC'15*, Richmond, VA, USA, May 2015, paper MOPTY056.
- [2] T. Kalvas, *et al*, "IBSIMU: A three-dimensional simulation software for charged particle optics", *Rev. Sci. Instrum.*, Vol. 81, 02B703, 2010.
- [3] M. S. Chung, T. E. Everhart, *J App Phys*, vol. 45, 1974, pp. 707-709, <http://dx.doi.org/10.1063/1.1663306>